



## Fabrication of biowaste derived carbon-carbon based electrodes for high-performance supercapacitor applications

Tadepalli Mitravinda<sup>a,b</sup>, Mani Karthik<sup>a</sup>, Srinivasan Anandan<sup>a</sup>, Chandra Shekar Sharma<sup>b\*</sup> & Tata Narasinga Rao<sup>a</sup>

<sup>a</sup> Centre for Nanomaterials, International Advanced Research Centre for Powder Metallurgy and New Materials, Hyderabad, Telangana 500 005, India

<sup>b</sup> Department of Chemical Engineering, Indian Institute of Technology Hyderabad, Kandi, Sangareddy Mandal, Hyderabad, Telangana 502 285, India

Received: 25 August 2020

The porous carbon is synthesised by chemical activation using cork dust bio-waste as carbon source and the electrochemical performance of the resulting carbon material is tested in even and uneven weight configuration using a two-electrode system. The obtained cork dust derived activated carbon (CDAC) shown a unique honeycomb structured morphology as confirmed by morphological analysis. X-ray diffraction (XRD) and Raman characterisation revealed the graphitic nature of the CDAC. Furthermore, the porous CDAC exhibited high specific surface area (1707 m<sup>2</sup>/g) and large pore volume (2.4 cc/g) with an average pore size of 4 nm. Even weight supercapacitor cell (SC) (positive and negative electrode with the same weight) and uneven weight SC cell (weight ratio of positive/negative electrodes:1.2) are assembled and tested in 1M TEABF<sub>4</sub>/AN. Uneven weight SC cell delivers the highest specific capacitance value of 107 F/g at a current density of 1 A/g. The uneven weight device shows promising cyclic stability without significant changes in capacitance values after 10000 and 5000 charge-discharge cycles at the potential window of 3 V and 3.2 V, respectively. On the contrary, a less specific capacitance (87 F/g at a current density of 1 A/g) observed for the even weight SC cell though high-capacity retention is realised under the same experimental conditions. The enhanced supercapacitor performance of uneven weight configuration SC cell is attributed to the weight balancing of the electrode, high graphitic nature, and unique pore size distribution with interconnected morphology of CDAC.

**Keywords:** Chemical activation, Supercapacitor, Even and uneven weight configuration, Weight balancing, Honeycomb

### 1 Introduction

Supercapacitors (SCs) with carbon-based porous electrodes are considered as attractive electrochemical energy storage systems for many applications<sup>1</sup>. They are often used for delivering high power over a short period. However, as compared to conventional batteries, the energy density stored in commercial carbon-based SCs is very less<sup>2</sup>. Hence, research activities were oriented towards increasing SCs energy density mostly by using aqueous and neutral electrolyte-based SC cells in view of widening the scope of applications that could use these devices.

The following formula defines the maximum energy density of the SC as a function of its capacitance (C) and operating voltage,

$$E = \frac{C \cdot V^2}{2 \cdot 3600} \quad \dots (2)$$

Two strategies were undertaken to improve the energy density, i.e., by addressing the inherent ability

of the active materials by enhancing the operating voltage window of the device. In the first strategy, the energy density of SCs was increased through pseudo faradaic reactions by loading functional groups on the surface of porous carbon<sup>3-6</sup>. The second approach was increasing the operating voltage of SCs based on the stability of electrolyte's potential window<sup>7</sup>.

#### 1.1 Even and uneven weight SC cell arrangement

There are two ways to fabricate the uneven weight type of SC cell; the first one includes two distinct carbon electrodes and the other way has a similar type of electrode material with disproportionate weights. The first way of fabricating uneven weight type SC cell is reported by many authors who used two distinct carbons having different textural characteristics<sup>8,9</sup>. The reports mention that the potential window of an aqueous electrolyte made SC cell is expanded to 1.6 V, while the neutral electrolyte can be increased to 2.2 V<sup>10-12</sup>. Whereas, the second way of SC cell fabrication has similar carbon materials having disproportionate weights. The second way of

\*Corresponding author  
(E-mail: cssharma@iith.ac.in, ch15resch11006@iith.ac.in)

fabrication is attractive and economically affordable since it needs just one carbon material<sup>11,12</sup>. Therefore, the expense of designing and processing the electrodes can be minimised. This method enables the weight balancing of positive and negative electrodes to maximise the operational potential window of the SC cell<sup>13</sup>. This method has been thoroughly tested in aqueous<sup>14,15</sup> and neutral based electrolytes<sup>12</sup> in which the potential window of electrolyte was extended from till 2.2 V. Commercially aqueous-based SC cells are used for different applications, but it has a lower energy density relative to organic electrolyte capacitors due to narrow electrochemical potential window. So, the industry generally uses organic electrolyte based SCs because of its high operating voltage, usually between 2.5 V and 2.85 V or above. Commercial electrochemical capacitors use an organic electrolyte, i.e., 1M organic electrolyte is prepared by solubilizing tetraethyl ammonium tetra fluoroborate (1 M TEABF<sub>4</sub>) salt either in acetonitrile (AN) or propylene carbonate (PC) organic solvents. The symmetrical (even weight of electrodes) double-layer capacitors comprise of electrodes containing same active material in equal quantities. However, balancing of the electrode weight is not the right choice when there is the same size of ions in the electrolyte (positive and negative ions) used. When the size of the electrolyte ions is different, electrode surfaces are not completely occupied by the ions if the same weight of the electrodes is used in the cell. So, the electrolyte ions are not fully used and could not contribute to the EDLC's overall capacitance. For example, in conventional TEABF<sub>4</sub> organic electrolyte, the sizes of the solvated cation (TEA<sup>+</sup>) and anion (BF<sub>4</sub><sup>-</sup>) are 0.68 nm and 0.48 nm, respectively. Since the anion is smaller, the electrode surface is occupied completely by these ions. In contrast, the surface of the other electrode could not occupy by these larger size cations. The excess ions (i.e., bigger cations) which could not occupy the electrode surface will not contribute to the overall capacitance<sup>16,17</sup>. Hence, fine-tuning electrode weight ratio with respect to the ionic size of electrolyte could result in ineffective usage of the entire surface of electrodes and thereby increases the overall capacitance of a super capacitor. The schematic illustration on the mechanism of even and uneven weight configuration of electrodes in an SC cell is described in Fig. 1.

### 1.2 Calculation of ion size ratio and electrode weight ratio

The purpose of this analysis is to establish the optimal electrode weight ratio and widen the voltage

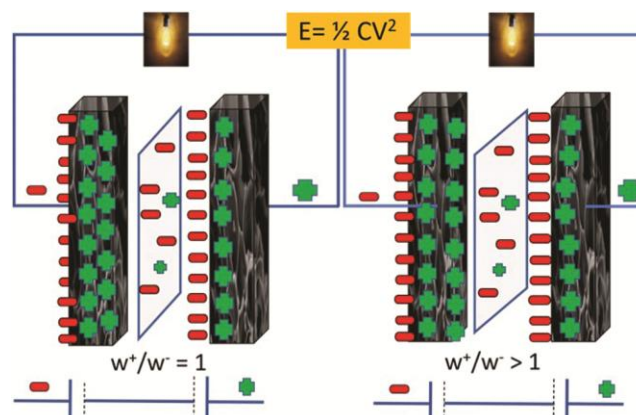


Fig. 1 — Mechanism of even and uneven weight configuration of electrodes in SC cell.

window of the EDLCs to increase the overall capacitance. The ratio of ion size and the ratio of theoretical electrode weight ratio are dependent on the size of hydrated electrolyte ions. The ionic size ratio is calculated for an electrolyte with the chemical compound form A<sub>x</sub>B<sub>y</sub> as:

$$\text{Ionic size ratio} = \frac{x \cdot r_A}{y \cdot r_B} \quad \dots (2)$$

where x is the number of ions A in the molecule, y is the number of ions B in the molecule, r<sub>A</sub> is the radius of solvated ion A, and r<sub>B</sub> is the radius of solvated ion B.

The conceptual electrode weight ratio is the reverse of the proportion of the ionic size:

$$\text{Theoretical electrode weight ratio} = \frac{y \cdot r_A}{x \cdot r_B} \quad \dots (3)$$

The electrode weight ratio of the EDLCs is determined as-

$$\text{Electrode weight ratio} = w^+ / w^- \quad \dots (4)$$

where w<sup>+</sup> is the weight of a positive electrode active ingredient and w<sup>-</sup> the weight of an active ingredient in a negative electrode<sup>16</sup>.

For instance, several researchers carried out an initial investigation of the mass balancing method to increase the operating voltage and capacitance of the EDLCs using aqueous and neutral electrolyte<sup>18-24</sup>. In the present study, we have attempted to optimize electrode weight ratio of each electrode to accommodate organic-based electrolyte ions (cations and anions) completely during electrochemical cycles, so that the energy density and capacitance could be increased by utilizing the maximum operational voltage window. The electrodes weight is balanced according to the size of the electrolyte ions (TEA<sup>+</sup> and

BF<sub>4</sub><sup>-</sup> ions) to completely use the surface of both the electrodes. Thus, the performance of supercapacitor derived from CDAC electrodes in non-aqueous electrolyte system (i.e. 1 M TEABF<sub>4</sub>/AN) is significantly increased to a higher potential window (3.2 V) in uneven weight configuration.

## 2 Experimental

### 2.1 Materials preparation

All the materials were used as such. Cork powder waste/cork dust (Advance Cork International, Karol Bagh, New Delhi) obtained from cork board was used as carbon source. High purity Tetra-ethyl ammonium-tetrafluoroborate (TEABF<sub>4</sub>, Sigma-Aldrich, 99%) salt is used to prepare organic electrolyte solution by dissolving in acetonitrile organic solvent in an argon atmosphere. Potassium hydroxide pellets (KOH, Fisher Scientific, 80%) was used as a chemical activation agent. Conducting activated carbon (YP-50F, Kuraray) was used to enhance the conductivity of the activated carbon.

### 2.2 Cork derived activated porous carbon as electrode material

Indigenous activated carbon with the high surface area was produced by chemical activation of cork dust with potassium hydroxide. Initially, cork dust (1 Wt.%) was combined with 3 wt.% of chemical activation agent potassium hydroxide (KOH) and dried for 12 hr. The resulting mixture was activated in a tubular furnace 900 °C for 1 hour with a heating rate of 5 °C min<sup>-1</sup> under nitrogen (N<sub>2</sub>) atmosphere. Finally, the resultant char was cleaned with distilled water and 1 M HCl solution to leach out K<sup>+</sup> ions completely from the activated carbon followed by drying at 80 °C for 12 hours.

### 2.3 Material Characterization

The structural features of carbon were analysed by powder X-ray diffraction (MXRD). Micro-area powder X-ray diffraction (MXRD) using Cu-K $\alpha$  ( $\lambda=1.5406$  Å) emission at 2 $\theta$  range varying from 10° to 80° at ambient temperature (MXRD, Smart lab micro area X-ray diffractometer, Micromax-007HF, Rigaku rapid-II). The degree of graphitization was analysed by using Raman spectrometer (Horiba Jobin Yvon - Lab Ram HR-800 Micro Raman Spectrometer) using an argon-ion laser as a light source at an excitation wavelength of 514 nm. Textural properties of (surface area, pore volume and pore size distribution) of carbon materials were

measured by Micro Metrics ASAP 2020 analyser using BET method<sup>25,26</sup>. The morphological features of the carbon material were analysed by scanning electron microscope (FE-SEM, Gemini 500, Zeiss) and transmission electron microscope (TECNAI-200 kV, FEI Netherlands). The elemental composition of the obtained carbon material was measured by a scanning electron microscope attached to the EDAX system (FE-SEM, Gemini 500, Zeiss). X-ray photoelectron spectroscopic (Omicron Nano Technology, UK) was carried out to analyse oxidation states and elemental composition of carbon material.

### 2.4 Electrochemical analysis

The electrochemical analysis of weight balanced SC cell was performed in a two-electrode configuration using 1M tetraethyl ammonium tetra fluoroborate in acetonitrile (1M TEABF<sub>4</sub>/AN) as electrolyte. An electrode slurry was prepared by adding cork dust derived nanoporous activated carbons, carbon black and PTFE (poly tetra fluoro ethylene) in the weight ratio of 80:10:10 w/w/w, respectively in ethanol to form a gel-like texture. Then the material was rolled on to form a free-standing electrode with intermittent addition of ethanol and later it was calendared on carbon-coated aluminium foil at 120 °C. The electrodes made were vacuum dried at 80 °C for 12 h followed by sintering into 12 mm diameter circular shape. The sintered electrodes were stacked together in even and uneven weight configuration (w+/w-:1, w+/w-:1.2) by a whatmann glass fibre separator wetted up by organic electrolyte in a glove box Potentiostatic Cyclic voltammetry (PCV), galvanostatic charge-discharge studies (GCD) and electrochemical impedance spectroscopy (10 kHz to 0.01 Hz) were performed for the resulting SC cells in AMETEK supplied PARSTAT 4000 workstation.

The gravimetric capacitance was measured according to the formulae (5)<sup>27,28</sup>.

$$C_{\text{cell}} = C_{2E}/4 \quad \dots (5)$$

$$C_{2E} = (2 \times I \times \Delta t) / (\Delta V \times m) \text{ (F/g)}$$

where,  $C_{\text{cell}}$  is the gravimetric capacitance of SC cell,  $I$  is the current discharged in a SC cell,  $\Delta V$  is the potential window of the SC cell,  $m$  is the mean mass of active materials on both electrodes.

The energy density and power density of the SC cell were calculated using the following Equations (6), (7):

$$E = (C_{\text{cell}} V^2) / (2 \times 3600) \quad \dots (6)$$

$$P = (E \cdot 3600) / t \quad \dots (7)$$

Where,  $C_{\text{cell}} = C_{2E}/4$  and  $E$  is the energy density,  $P$  is the power density,  $V$  is the cell voltage, and  $t$  is the time taken for discharge, respectively<sup>29</sup>.

### 3 Results and Discussion

#### 3.1 The mechanism for the formation of cork activated carbon

Different steps are involved in producing KOH activated nano-porous carbon from cork dust. As described in the experimental section, the chemical activation process produces nanoporous carbon by using cork dust as a carbon source. The chemical activation includes various physical and chemical changes at high temperatures when the cork dust was treated with potassium hydroxide and eventually the potassium ion was hosted on the carbon grid structure, which contributes to the formation of nanoporous activated carbon after removal of potassium ion from carbon grid<sup>30</sup>. The in-situ potassium ions would possibly undergo several decomposition steps, followed by the creation of pores and enlargement of pores at high temperatures. The mechanism for the formation of activated carbon with nanoporous structure through KOH based chemical activation was discussed in detail in our previous paper<sup>25</sup>.

#### 3.2 Characterisation of carbon materials

The XRD pattern of CDAC in Fig. 2a shows diffraction peaks at  $2\theta$  values of  $26^\circ$  and  $44^\circ$  revealing the graphitized nature of carbon after chemical activation<sup>31</sup>. Generally, the (002) XRD reflection at  $26^\circ$  attributes to the presence of polycyclic aromatic carbon sheets of amorphous carbon in irregular orientation, while (100) the reflection appeared at  $44^\circ$  attributes to the presence of 2D in-plane diffraction of graphene sheets<sup>32</sup>. The degree of graphitisation was further investigated by Raman spectroscopic analysis and the results are shown in Fig. 2b. The two prominent peaks at  $1356 \text{ cm}^{-1}$  and  $1596 \text{ cm}^{-1}$  (Fig. 2b) represents disordered amorphous carbon and ordered graphitic

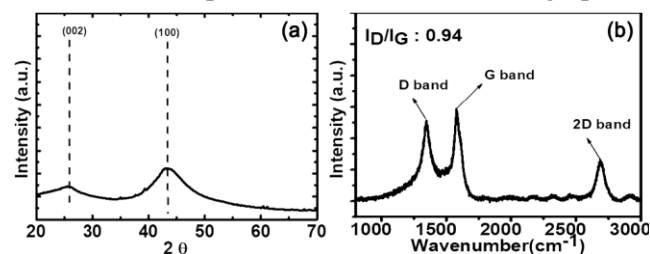


Fig. 2 — (a) X-ray diffraction of the CDAC and (b) Raman Spectra of the CDAC.

$sp^2$ -hybridized carbon, respectively. D band can occur in all amorphous and nanocrystalline carbon due to defects or small crystallite sizes<sup>33</sup>. The G band corresponds to the doubly degenerate  $E_{2g}$  phonons in the Brillouin region that emerges from the first-order Raman scattering process<sup>34–36</sup>. The ratio of the intensity of the D band and intensity of G band ( $I_D / I_G$ ) implies graphitisation level; a lower  $I_D / I_G$  ratio represents a higher degree of graphitisation. The  $I_D/I_G$  ratio of cork derived activated carbon is considerably lower (0.94) than the commercially available carbon ( $I_D/I_G$  ratio 1.92). It is consistent with the results of the XRD<sup>37</sup>, indicating high crystallinity of CDAC. Further, the peak also appears at  $2684 \text{ cm}^{-1}$  attributes to the process of second-order double resonance associated with the phonons of zone boundary<sup>38</sup>. Two-boundary phonons are involved in the scattering process of 2D mode whereas a phonon and a defect are involved in D mode. In comparison to the D band, which includes defects in the scattering process, the 2D band does not need defects. The 2D band is therefore evident in the few-layered Raman spectrum.

The microstructure shows that the cork derived activated carbon (CDAC) was an interconnected porous structure and the Transmission electron microscopy (TEM) image displayed the presence of micropores. The SEM image shown in Fig. 3a revealed the presence of honeycomb structured carbon domains with a diameter of 100 micrometres. After the potassium hydroxide chemical activation,

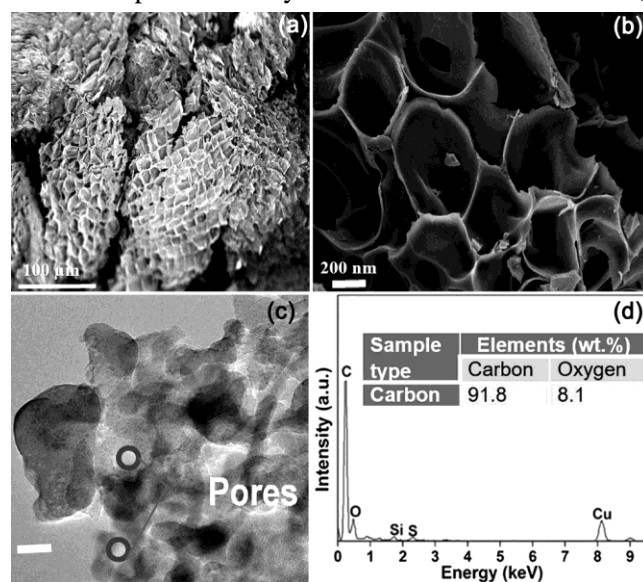


Fig. 3 — FESEM image of (a) Raw cork, (b) cork derived activated carbon and TEM image of (c) cork derived activated carbon (CDAC) (d) EDAX OF cork derived activated carbon (CDAC).

the honeycomb-like morphology was well retained in CDAC, as shown in Fig. 3b. TEM image shows that the carbon sheet thickness was reduced from 100  $\mu\text{m}$  to 100 nm after activation. The reduction in carbon sheet thickness is attributed to a significant volume of carbon being lost during the KOH activation. The pore size of the pores observed on the surface of CDAC measured by TEM analysis was 10 nm, as shown in Fig. 3c. Furthermore, the honeycomb structured CDAC's become much more flexible, and numerous wrinkles were found on the surface of CDAC. The activation by KOH is expected to generate large micropores on the carbon surface which will be discussed in BET discussion. The unique honeycomb-like morphology obtained after the chemical activation is beneficial for EDLC application as it can offer interconnected pathways for both electrolyte penetration and electrolyte mobility<sup>39</sup>. In addition, the interconnected microporous network will have uniform pore size and exhibit high electrical conductivity across the electrode of the capacitor. Further, EDAX elemental analysis was carried out to know the atomic percentage of elements present in the carbon. The spectrum of CDAC shows the existence of carbon, oxygen and a slight amount of silica, as shown in Fig. 3d. Elemental analysis shows the

presence of 91.8 % carbon and 8.1 % oxygen, as presented in the Table included in Fig. 3d.

The oxidation states and the exact atomic percentage of elements present in the carbon are evaluated from the X-ray photoelectron spectroscopy (XPS). The XPS survey spectrum of CDAC shows the existence of C1s, O1s spectrum, as described in Fig. 4(a-c). Elemental analysis shows the presence of 91.2 % carbon and 8.8 % oxygen. The atomic percentage of oxygen (8.8%) was due to the thermally stable oxygen functional groups adsorbed on the surface of the CDAC material. The high-resolution C1s spectra of CDAC can be resolved into three component peaks centred at 284.6 eV, 285.3 eV, and 285.9 eV, corresponding to  $\text{Csp}^2\text{-Csp}^2$ ,  $\text{N-Csp}^2$ , and  $\text{N-Csp}^3$  bonds, confirming the presence of high percentage of  $\text{sp}^2$  carbon which is consistent with XRD and Raman analysis.

A nitrogen adsorption-desorption measurement assessed the surface area and pore size distribution of the activated carbon material. The Nitrogen adsorption-desorption isotherms and pore size distribution of CDAC material are shown in Fig. 5a and Fig. 5b. It is evident that a carbon sample exhibit a type I Isotherm indicating the presence of hierarchical micro to mesoporous characteristics of

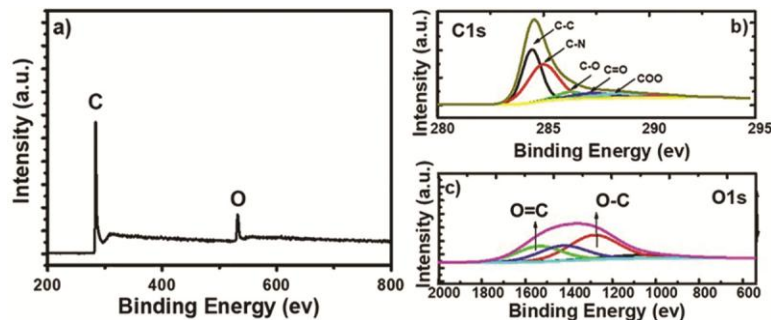


Fig. 4 — (a-c) X-ray photoelectron spectroscopy of cork activated carbon.

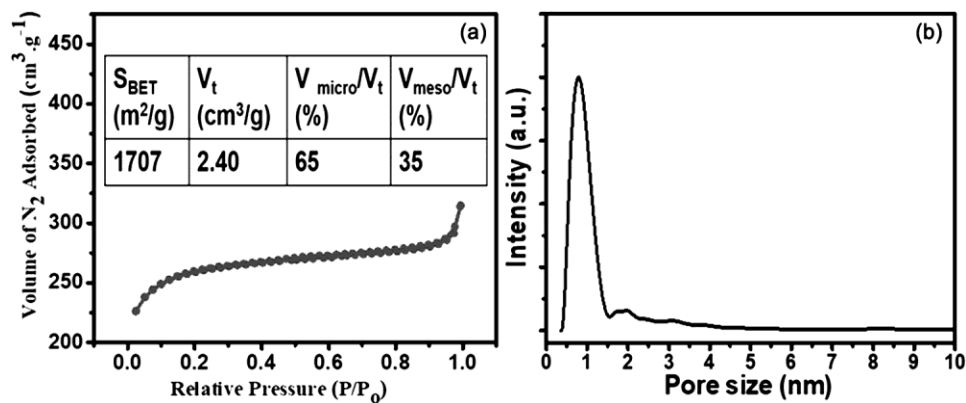


Fig. 5 — (a) Nitrogen adsorption-desorption studies and (b) The pore size distribution of activated carbons.

carbon. The isotherm of CDAC exhibits a sharp increase at a low relative pressure region indicating the presence of highly microporous nature of carbon. A detailed summary of the results of specific surface area ( $S_{\text{BET}}$ ), total pore volume ( $V_{\text{total}}$ ), and average pore diameter ( $D_p$ ) of carbon sample are presented in the Table included in Fig. 5a. CDAC has a comparatively large specific surface area of  $1707 \text{ m}^2/\text{g}$ , which is due to the porosity created by KOH activation<sup>40</sup>. CDAC also features a hierarchical micro/mesoporous network with high microporous specific surface area ( $S_{\text{micropore}}$ ) of  $1637 \text{ m}^2/\text{g}$  and total pore volume of  $2.4 \text{ cm}^3/\text{g}$ . The findings from T-plot also show that the average pore volume is  $2.4 \text{ cm}^3/\text{g}$  and the specific surface area is  $1707 \text{ m}^2/\text{g}$  with a high microporous surface area of  $1637 \text{ m}^2/\text{g}$ . Upon further calculation, 65% microporous volume and 35% of the mesoporous volume are quantitatively analysed. The pore diameter of 4.2 nm is investigated from the pore size distribution of activated carbon, as shown in Fig. 5b. The observed high specific surface area of activated carbon, with a hierarchical micro-mesoporous framework and narrow pore size distribution, could provide an extensive interaction of electrodes with electrolyte. It was reported that the carbon with the above structural and textural features would enhance

the electrochemical performance and rate capability as they influence ionic diffusion through electrolyte and electrode interface. Aligning with the above observation, in the present study, CDAC is expected to deliver improved performance due to its excellent structural parameters such as high specific surface area, narrow pore size distribution, large pore volume and graphitic nature.

### 3.3 Electrochemical performance of carbon materials

The electrochemical performance of supercapacitor fabricated with activated carbon was studied in even and uneven weight configurations ( $w^+/w^-:1$  and  $w^+/w^-:1.2$ ) of electrodes using Potentiostatic cyclic voltammetry study at different scan rates, Galvanostatic charge-discharge study at different current densities and electrochemical impedance spectroscopy techniques. The PCV and GCD curves of the supercapacitor device with organic electrolyte (1M TEABF<sub>4</sub>/AN) in an even and uneven weight configuration were examined at different voltage windows (2.7 V, 3 V and 3.2 V) at different scan rates and different current densities as shown in the Fig. 6 & Fig 7. As reported in the literature that the rapid scan rate of 20 mV/s was chosen to sustain the discharge times in minutes and to represent the efficiency of the SC performance<sup>28</sup>.

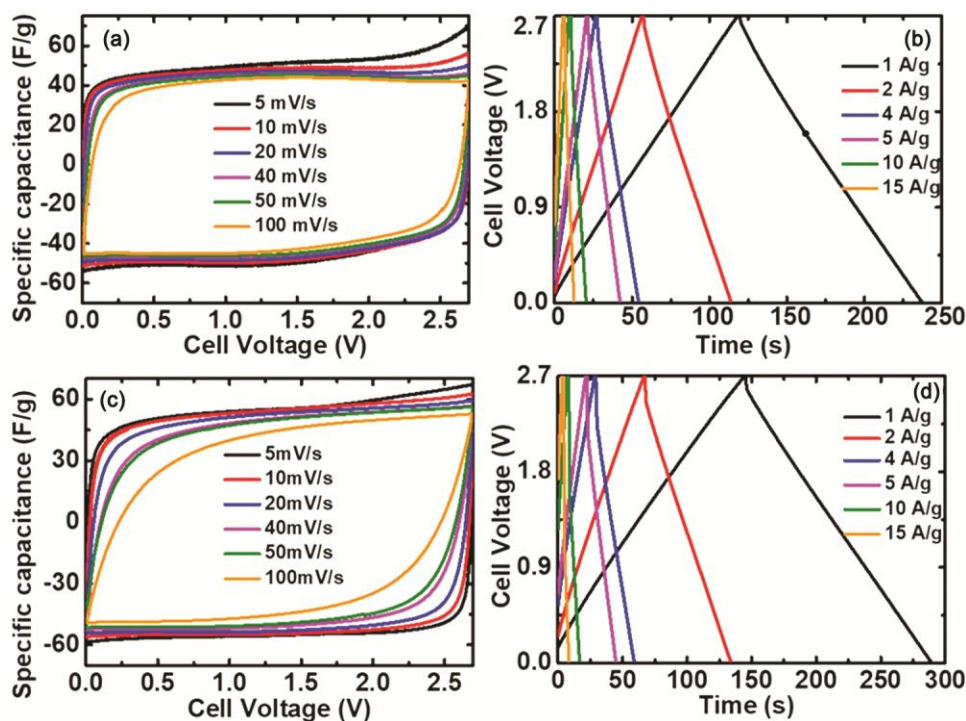


Fig. 6 — (a) & (c) Potentiostatic cyclic voltammograms of even and uneven weight capacitor at various scan rates and (b) & (d) Galvanostatic Charge/discharge curves of even and uneven weight capacitor at different current densities.

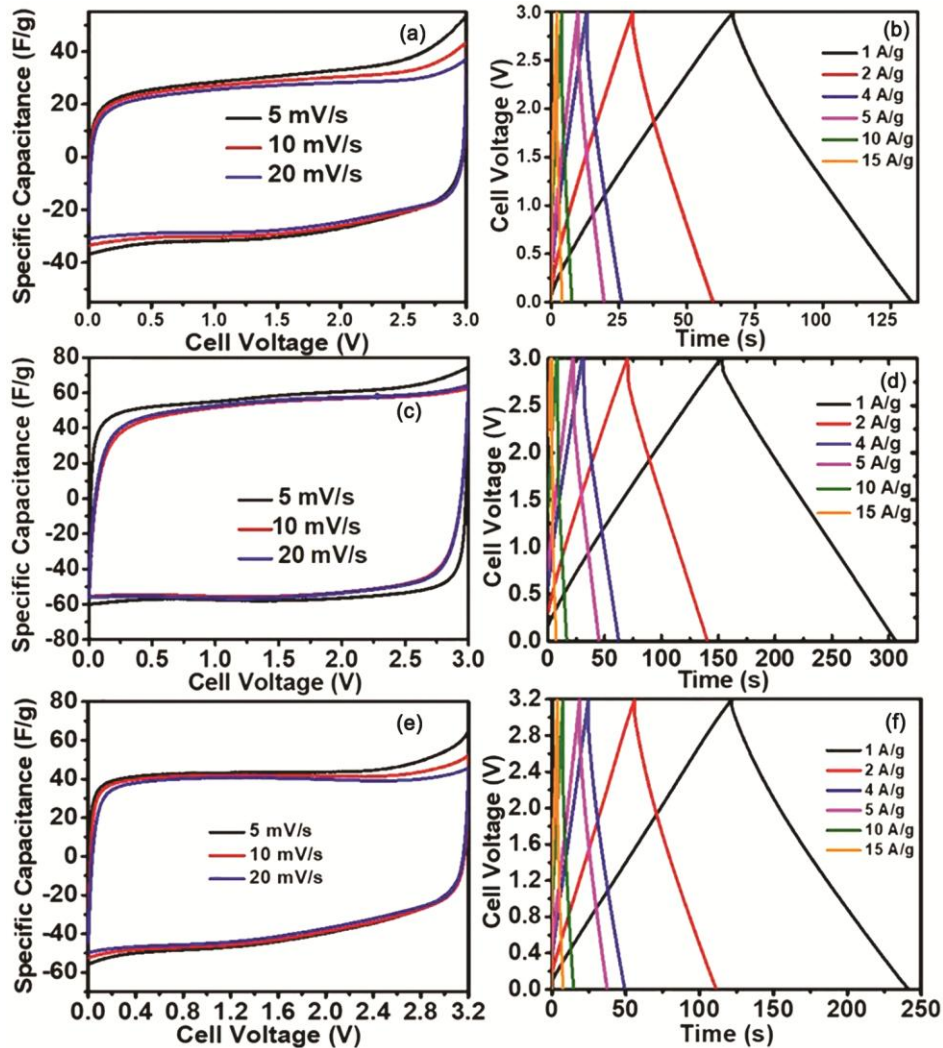


Fig. 7 — (a) & (c) cyclic voltammograms of even and uneven weight capacitor at different scan rates at 3 V, (b) & (d) Galvanostatic Charge/discharge curves of even weight SC cell at various current densities at 3 V, (e) cyclic voltammograms of uneven weight capacitor at different scan rates at 3.2 V and (f) Galvanostatic Charge/discharge curves of uneven weight SC cell at various current densities at 3.2 V.

### 3.3.1 Electrochemical characterisation of even and uneven weight configuration tested from 0 V to 2.7 V

Figure 6a showed that the CV curves of the SC cell made from Cork dust activated carbon (CDAC) in even weight configuration ( $w^+/w^-:1$ ) exhibit a rectangular shape when tested at voltage window of 0 V to 2.7 V. Also, the CV curves exhibit a distortion or quasi-rectangular form at a higher scan rate of 20 mV/s, indicating its poor rate capability. Further, the specific capacitance at different current densities is studied through GCD data to investigate the rate capability of an EDLC. As illustrated in Fig. 6b, the specific capacitance of even weight configuration was carried out by GCD curves tested at various current densities from 0.5 A/g to 15 A/g. As shown in Fig. 6b

the even weight supercapacitor device exhibits triangular shapes which are in the isosceles form. The specific capacitance of CDAC electrode SC cell with even weight configuration calculated from GCD is 87 F/g at 1 A/g current density when tested at 0 to 2.7 V. Furthermore, with the increase in current density upto 15 A/g, a decrease in the gravimetric capacitance to 67 F/g is observed with an IR drop observed in the charge-discharge curve is around 0.25 V. From Fig. 6c, it is observed that the CV curves of CDAC electrode SC cell with uneven weight configuration ( $w^+/w^-: 1.2$ ) exhibit a rectangular shape at both slower and faster scan rates indicating the typical behaviour of an EDLC. The rectangular shape is well preserved even at higher scan rates, which indicates the

electrochemical stability window of the electrolyte. Thus, the CV profile concludes that CDAC electrode SC cell with uneven weight configuration has demonstrated stable electrochemical capacitor behaviour compared to the CDAC electrode SC cell with even weight configuration.

Rate capability is one of the main parameters affecting EDLC's performance that rely on the material characteristics, electrical characteristics and ionic mobility through the porous channels of carbon. As shown in the Fig. 6d, uneven weight configuration SC cell exhibit an isosceles triangle shape with low IR drop, suggesting an ideal EDLC behaviour. The specific capacitance of CDAC electrode SC cell with uneven weight configuration calculated from GCD curve showed an excellent gravimetric capacitance of 107 F/g at 1 A/g current density tested from 0 V to 2.7 V. Furthermore, CDAC electrode SC cell exhibits gravimetric capacitance of 74 F/g at a high current density of 15 A/g with IR drop observed in a charge-discharge curve is around 0.1 V. The GCD profile of CDAC electrode SC cell with uneven weight configuration is more stable with less capacity retention compared to the CDAC electrode with even weight configuration.

### 3.3.2 Electrochemical characterisation of even and uneven weight configuration tested from 0 V to 3 V and 0 to 3.2 V

To further validate the difference in performance, PCV and GCD studies were carried out on CDAC electrode SC cell with both even and uneven weight configurations at different scan rates and current densities in the voltage range of 0 V to 3.0 V and 0 V to 3.2 V. Figure 7a shows the PCV profile of CDAC electrode SC cell with even weight configuration ( $w+/w-: 1$ ) at different scan rates. With an increase in scan rate, the capacitance decreases. As shown in Fig. 7a, the PCV curves of EDLC SC cell with even weight configuration show a rectangular form without any distortion till 2.7 V. In the PCV curves, post 2.7 V, distortion behaviour is observed due to poor electrolyte's potential stability. Also, the CV curves exhibit a distortion or quasi-rectangular shape even at 20 mV/s scan rate, indicating the poor rate capability. Figure 7b shows GCD curves of CDAC electrode SC cell with even weight configuration ( $w+/w-: 1$ ) tested at a potential window of 0 V to 3 V. The curves observed to have a non-isosceles triangle in shape indicating poor electrochemical stability of the electrolyte and poor rate capability. The specific capacitance of CDAC material is calculated from the

discharge time obtained at various current densities. A gravimetric capacitance of 80 F/g is observed at 1 A/g current density and 54 F/g at a higher current density of 15 A/g indicating high-capacity retention. Figure 7c shows the PCV curves of uneven weight ( $w+/w-: 1.2$ ) SC cell having broader rectangular PCV shapes without any faradaic effects indicating an ideal behaviour of the EDLC SC cell. Further, the rectangular PCV curves are remained without any distortion even at a higher scan rate of 20 mV/s, demonstrating fast charge-discharge cycles of the EDLC SC cell. These results suggest that CDAC electrode SC cell with uneven weight configuration ( $w+/w-: 1$ ) shows higher capacitance, rate capability and reversibility nature even at higher scan rates confirming electrolyte's potential stability. To further analyse the potentiality of uneven weight CDAC electrode SC cell, it was measured at different current densities from 0 to 3 V potential window by GCD curves which are presented in Fig. 7d. The charge-discharge curves observed to have 103 F/g of specific capacitance calculated from the discharge time exhibited at a current density of 1 A/g. Upon an increase in the current density to 15 A/g, the specific capacitance is found to be 61 F/g, which indicates lower capacity retention. In addition, to analyse the capability of uneven weight SC cell, it was tested at 0 to 3.2 V potential window. CV curves of CDAC electrode SC cell with uneven weight configurations exhibit a rectangular shape with no distortion is observed even at low scan rates indicating its ideal behaviour. As shown in Fig. 7e, the rectangular form was well maintained until 3.2 V, indicating the electrolyte's potential stability. To confirm further, the CDAC electrode SC cell with uneven weight configuration was systematically tested by GCD curves at 3.2 V, which exhibit an ideal behaviour with less IR drop (Fig. 7f). The specific capacitance of electrodes was calculated from GCD curves. The specific capacitance of CDAC electrode SC cell with uneven weight configuration at 1 A/g current density was observed to be 101 F/g and at a higher current density of 15 A/g it is 60 F/g. Whereas, the specific capacitance of commercial YP 50 SC cell at a current density of 15 A/g was observed to be 34 F/g.

As supported by several research groups<sup>41</sup>, even weight (same weight) carbon/carbon-based SC cell showed an excellent rate capability and EDLC behaviour at 2.7 V. Whereas, when the cell voltage increases up to 3.2 V, the distortion or quasi-

rectangular shape with poor rate capability observed is due to the imbalance in potential distribution between the two electrodes. A decrease in the cyclic stability of the SC cell was also observed because one of the electrodes operate at a potential beyond the electrolyte stability limit. From the results, it is evident that the voltage window of CDAC electrode SC cell with even weight configuration is only up to 2.7 V.

The SC cell with uneven electrode weight configuration operates at a higher potential window than that of even weight type due to uniformly distributed potential among the two electrodes. Hence, equilibrium was attained between those electrodes resulting in the expansion of electrolyte potential window for uneven weight type ( $w^+/w^-: 1.2$ ) of EDLC device that exhibits higher energy density, power density and low IR drop ( $w^+/w^-: 1$ )<sup>11</sup> suggesting a very low equivalent series resistance (ESR) than the even weight SC cell. It can be seen from the Figures, that the Isosceles triangular curves with lower IR drops were observed only for the uneven weight configuration indicating an ideal EDLC behaviour with reversibility nature and higher Coulombic efficiency.

To clearly distinguish the performance of even and uneven weight SC cell, comparison graphs

were plotted with respect to PCV, GCD, EIS and cyclic stability, as shown in Fig. 8. Figure 8a shows the comparison of electrochemical impedance spectroscopy of even and uneven weight SC cell. The impedance characteristics like solution resistance ( $R_s$ ),  $R_{ct}$  (charge transfer resistance) and diffusion resistance are analysed. The  $R_s$  (solution resistance) and  $R_{ct}$  are calculated to be 3.47  $\Omega$  and 4.7  $\Omega$ , respectively for even weight SC cell whereas for the uneven weight SC cell.  $R_s$  (solution resistance) and  $R_{ct}$  are 1.6  $\Omega$  and 4.2  $\Omega$ , respectively. The sum of  $R_s$  and  $R_{ct}$  is known to be equivalent series resistance which is lower for uneven weight SC cell than even weight SC cell indicating the high performance of uneven weight SC cell. The comparison of PCV curves of CDAC electrode SC cell with even and uneven weight configurations exhibit rectangular shape even at low scan rates representing the ideal behaviour of the EDLC with uneven weight configuration as shown in the Fig. 8b. The even weight SC curve shows slight distortion beyond 2.7 V because of poor electrolyte potential stability. Also, the uneven weight curve exhibits a rectangular shape with no distortion up to 3.2 V, indicating an increase in the electrolyte's potential stability.

Also, the even and uneven weight configuration were compared systematically by GCD curves which

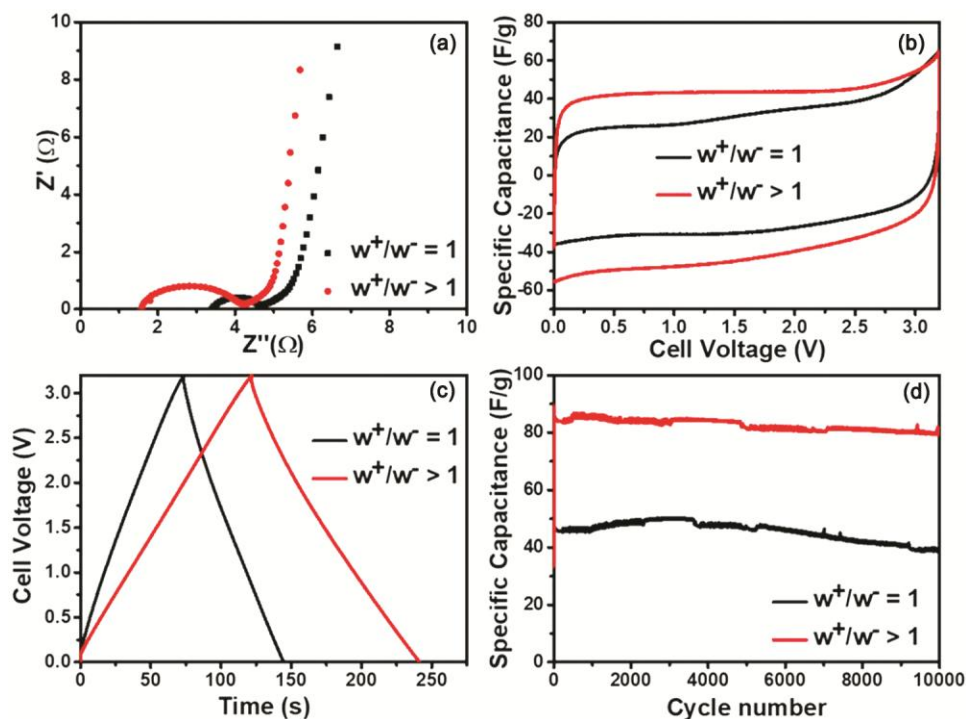


Fig. 8 — Comparison of (a) electrochemical impedance spectroscopy, (b) CV profile and (c) CD profile and (d) Cyclic Stability study of even weight and uneven weight capacitors.

exhibit an ideal behaviour of EDLC capacitor, as shown in Fig. 8c. The gravimetric capacitance of electrodes was calculated using discharge time obtained from the GCD cycle. As seen in the charge-discharge curve with a potential window of 0 to 3.2 V, the activated carbon electrode with uneven weight configuration exhibit an excellent gravimetric capacitance of 101 F/g at 1 A/g current density. Furthermore, it exhibits a gravimetric capacitance of 60 F/g at a high current density of 15 A/g with lower IR drop of 0.1 V indicating a very low ESR. Whereas, the Commercial SC cell made of YP-50 electrode material exhibit capacitance of 34 F/g (25 F/cm<sup>3</sup>) at a current density of 15 A/g<sup>19</sup>. The comparison of specific capacitance at different current densities of even and uneven weight SC cell at 2.7 V, 3V and 3.2 V are presented in Table 1.

The stability of the electrode in CDAC SC cell with even and uneven weight configurations was assessed with a long-term cyclic study at 4 A/g current density. It was observed that in uneven weight system, the capacitance remained above ~94 % of its initial value with a less equivalent series resistance (ESR) even after 10,000 cycles, evidencing a stable performance of the CDAC electrode. Whereas, even weight electrode device is stable till 5000 cycles are showing capacity retention of only ~85 % of its initial capacitance.

The rapid charge-discharge profile with high ESR shown in the Fig. 8d indicates degradation of even weight electrodes and so the specific capacitance was observed to be decreased after 5000 cycles. The obtained results are in good agreement with the published literature<sup>23</sup>, wherein a decrease in the cyclic stability of SC cell was observed when the even weight configuration carbon electrodes are used because one of the electrodes operate at a potential

beyond the electrolyte stability limit. Whereas, a smart adjustment of active material weight ratio of electrodes in uneven weight configuration SC cell leads to the complete utilization of the voltage window of each electrode thereby increasing the operating voltage and energy density of the SC cell. The electrochemical characterization shows the better performance of weight balanced uneven weight configuration showing high energy density of 26.8 Wh/Kg till voltage window of 3.2 V, less solution resistance, higher specific capacitance with excellent cyclic stability in comparison with even weight configuration. The energy density and power density of CDAC carbon in uneven weight configuration are compared with other asymmetric carbon / uneven weight configured SC cells reported earlier, as shown in the Ragone plot presented in Fig. 9. The enhanced Supercapacitor performance of uneven weight configuration is attributed to the weight balancing of the electrodes, high graphitic nature, narrow pore size distribution and unique interconnected morphology of the activated carbon.

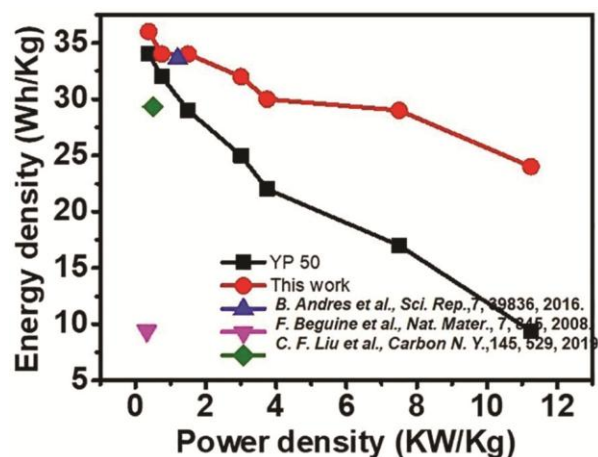


Fig. 9 — Ragone plot.

Table 1 — Comparison of specific capacitance of even and uneven weight SC cell at 2.7 V, 3 V and 3.2 V

Current density (A/g)	2.7 V		3 V		3.2 V
	Even weight SC gravimetric capacitance (F/g)	Uneven weight SC gravimetric capacitance (F/g)	Even weight SC gravimetric capacitance (F/g)	Uneven weight SC gravimetric capacitance (F/g)	Uneven weight SC gravimetric capacitance (F/g)
0.5	90	113	83	108	107
1	87	107	80	103	101
2	83	98	74	94	93
4	80	85	68	81	80
5	78	81	63	74	73
10	74	79	59	66	63
15	67	74	54	61	60

#### 4 Conclusions

By changing from an even weight configuration to an optimal electrode weight ratio of 1.2, an increase in specific capacitance and improvement of the performance of SC cell were observed with respect to cell voltage and cycle life. The even/uneven electrode configurations of cork derived CDAC SC cell was successfully examined using a non-aqueous electrolyte (i.e. 1M TEABF<sub>4</sub>/AN) to know the effect of electrode weight ratio on the performance of SC cell. The electrochemical results reveal that uneven weight configuration exhibits the excellent performance of SC cell with respect to high capacitance, good rate capability and long cyclic stability than the even weight configuration of an electrochemical capacitor, attributed to the excellent structural parameters such as high surface area, narrow pore size distribution and large pore volume and graphitic nature of CDAC.

#### Acknowledgement

The authors are thankful to Mr. G. Padmanabham, Director of ARCI, for his support in carrying out the work. The research work is supported by ARCI - technical research centre (Ref. No. AI/1/65/ARCI/2014(C)) through the Department of Science and Technology (DST), Government of India, New Delhi, India is highly acknowledged.

#### References

- Simon P & Gogotsi Y, *Nat Mater*, 7 (2008) 845.
- Zuo W, Li R, Zhou C, Li Y, Xia J & Liu J, *Adv Sci*, 4 (2017) 1600539.
- Khomenko V, Raymundo P E & Beguin F, *J Power Sources*, 195 (2010) 4234.
- Ra E J, Raymundo P E, Lee Y H & Beguin F, *Carbon N Y*, 47 (2009) 2984.
- Bleda Martinez M J, Macia Agullo J A, Lozano Castello D, Morallon E, Cazorla Amoros D & Linares Solano A, *Carbon N Y*, 43 (2005) 2677.
- Pech D, Guay D, Brousse T & Belanger D, *Electrochim Solid-State Lett*, 11 (2008) A202.
- Andres B, Engstrom A C, Blomquist N, Forsberg S, Dahlstrom C & Olin H, *Sci Rep*, 7 (2016) 39836.
- Choudhary N, Li C, Moore J, Nagaiah N, Zhai L, Jung Y & Thomas J, *Adv Mater*, 29 (2017) 1605336.
- Wang H, Holt Chris M B, Li Z, Tan X, Shalchi Amirkhiz B, Xu Z, Olsen B C, Stephenson T & Mitlin D, *Nano Res*, 9 (2012) 605.
- Li J, Tang J, Yuan J, Zhang K, Sun Y, Zhang H & Qin L C, *Electrochim Acta*, 258 (2017) 1053.
- Chae J H & Chen G Z, *Electrochim Acta*, 86 (2012) 248.
- Gao Q, Demarconnay L, Raymundo Pinerio E & Francois B, *Energy Environ Sci*, 5 (2012) 9611.
- Chmiola J, Largeot C, Taberna P L, Simon P & Gogotsi Y, *Angew Chemie - Int. Ed*, 47 (2008) 3392.
- Hu L, Guo D, Feng G, Li H & Zhai T, *J Phys Chem C*, 120 (2016) 24675.
- He T, Ren X, Nie J, Ying J & Cai K, *Int J Electrochem*, (2015) 1.
- Andres B, Engstrom A C, Blomquist N, Forsberg S, Dahlstrom C & Olin H, *Sci Rep*, 7 (2016) 39836.
- Vaquero S, Palma J, Anderson M & Marcilla R, *Int J Electrochem Sci*, 8 (2013) 10293.
- Brandt A, Isken P, Lex Balducci A & Balducci A, *J Power Sources*, 204 (2012) 213.
- Vijayakumar M, Rohita D S, Rao T N & Karthik M, *Electrochim Acta*, 298 (2019) 347.
- Gao Q, *Optimizing carbon/carbon supercapacitors in aqueous and organic electrolytes, Ph D thesis, University of Orleans*, (2013).
- Cericola D, Kotz R & Wokaun A, *J Power Sources*, 196 (2011) 3114.
- Biswal M, Banerjee A, Deo M & Ogale S, *Energy Environ Sci*, 6 (2013) 1249.
- Beguin F & Elzbieta F, *Carbons for Electrochemical Energy Storage and Conversion Systems, (CRC Press, New York), 1st Edn, ISBN:978-1-4200-5307-4, (2009)*.
- Liu C F, Liu Y C, Yi T Y & Hu C C, *Carbon N Y*, 145 (2019) 529.
- Mitravinda T, Nanaji K, Anandan S, Jyothirmayi A, Chakravadhanula V S K, Sharma C S & Rao T N, *J Electrochem Soc*, 165 (2018) A3369.
- Mandzyuk V, Lisovskyy R & Nagirna N, *Nanosci Nanotechnol Res*, 1 (2013) 23.
- Mahmood A, Zou R, Wang Q, Xia W, Tabassum H, Qiu B & Zhao R, *ACS Appl Mater Interfaces*, 8 (2016) 2148.
- Stoller M D & Ruoff R S, *Energy Environ Sci*, 3 (2010) 1294.
- Yu D, Goh K, Wang H, Wei L, Jiang W, Zhang Q, Dai L & Chen Y, *Nat Nanotechnol*, 9 (2014) 555.
- Yoon S H, Lim S, Song Y, Ota Y, Qiao W, Tanaka A & Mochida I, *Carbon*, 42 (2004) 1723.
- Guo H & Gao Q, *J Power Sources*, 186 (2009) 551.
- Ong T S & Yang H, *Carbon*, 38 (2000) 2077.
- Chu P K & Li L, *Mater Chem Phys*, 96 (2006) 253.
- Jiang X F, Wang X Bin, Dai P, Li X, Weng Q, Wang X, Tang D M, Tang J, Bando Y & Golberg D, *Nano Energy*, 16 (2015) 81.
- Ferrari A C & Robertson J, *Philos Trans R Soc A Math Phys Eng Sci*, 362 (2004) 2477.
- Ferrari A C & Robertson J, *Am Phys Soc*, 64 (2001) 1.
- Wang H, Xu Z, Kohandehghan A, Li Z, Cui K, Tan X, Stephenson T J, King Ondu C K, Holt Chris M B, Olsen B C, Tak J K, Harfield D, Anyia A O & Mitlin D, *ACS Nano*, 7 (2013) 5131.
- Wang H, Maiyalagan T & Wang X, *J Am Chem Soc Catal*, 2 (2012) 781.
- Vijayakumar M, Adduru J, Rao T N & Karthik M, *Glob Challenges*, 2 (2018) 1800037.
- Guo Z, Zhou Q, Wu Z, Zhang Z, Zhang W, Zhang Y, Li L, Cao Z, Wang H & Gao Y, *Electrochim Acta*, 113 (2013) 620.
- Wang D, Fang G, Geng G & Ma J, *Mater Lett*, 189 (2017) 50.